Norfloxacin removal from aqueous solution using biochar derived from *luffa* sponge

Yu Feng, Qian Liu, Yang Yu, Qiang Kong, Lu-lu Zhou, Yuan-da Du and Xiao-feng Wang

ABSTRACT

This study addresses the absorbance of norfloxacin (NOR) in wastewater by biochar derived from *luffa* sponge. Observations using scanning electron microscopy (SEM) show that the adsorbent surface is coarse with a heterogeneous, irregular, and highly porous structure. The calculated Brunauer-Emmett-Teller (BET) surface area of the adsorbent is 822.35 m^2/g with an average pore size of 5.35 nm. In the experiments, the biochar (BC) adsorbed 99.86% of the NOR with a maximum absorption of approximately 250 mg/g. The correlation coefficient ($R^2 > 0.99$) for the Freundlich simulation indicates multimolecular layer adsorption. The pseudo-second-order model ($R^2 = 0.9998$) indicates that chemisorption involving valence forces through the exchange or sharing of electrons controls the adsorption rate. A negative enthalpy change confirms endothermic adsorption. Fourier-transform infrared (FTIR) spectroscopy analysis indicates that the BC surface contains more acidic oxygen-containing groups, such as carboxyl, phenol hydroxyl, lactone, and carbonyl. These findings demonstrate that *luffa* sponge biochar can efficiently remove NOR from aqueous solutions. Additionally, the use of *luffa*, which is a natural biological material, can help to reduce waste and provide a new source of BC for wastewater treatment of antibiotic residues.

Key words | adsorption, isotherm, kinetic, thermodynamic

Yu Feng†
Qian Liu†
Qiang Kong (corresponding author)
Lu-lu Zhou
Yuan-da Du
Xiao-feng Wang
College of Geography and Environment,
Collaborative Innovation Center of Human-Nature and Green Development in Universities of Shandong,
Shandong Normal University,
Jinan 250014,
China
E-mail: *kongqiang0531@hotmail.com*

Yang Yu
National Facility for Protein Science in Shanghai,
ZhangJiang Lab,
Shanghai Advanced Research Institute, Chinese Academy of Sciences,
Shanghai, 201210,
China

†These authors contributed equally to this work.

INTRODUCTION

Pharmaceutical and personal care products (PPCPs) are a new type of widely produced trace pollutants that have become a global environmental problem and, accordingly, an active topic in dangerous material pollution and prevention research. Antibiotics are the most frequently detected PPCPs worldwide and the third most common drugs used in modern medicine, accounting for more than 6% of all prescription drugs (Boerner *et al.* 2003) after veterinary drugs, which account for more than 70% (Hallingsørensen *et al.* 1998). However, about 25–75% of animal-based drugs are excreted after being absorbed in metabolites and drug-targeted organs, such that the quantity and structure of antibiotic species in wastewater is rapidly becoming more numerous and complex. Such antibiotic contamination can increase microbial resistance, which can indirectly affect human health by causing a decline of the body's immune system capacity and increased allergic reactions (Kong *et al.* 2016).

Norfloxacin (NOR) is a ubiquitous antibiotic in the natural environment that is commonly used to treat enteritis dysentery because of its effectiveness against the DNA rotation enzymes (DNA gyrase) of pathogenic bacteria in the digestive tract (Holmes *et al.* 1985). Although environmental NOR concentrations are low, its chemical structure has specific biological implications with the potential to create cumulative adverse effects on non-target organisms.

doi: 10.2166/aqua.2018.040

The removal of residue from the water is therefore necessary. Several methods to achieve NOR degradation (e.g., sonophotocatalytic degradation, ozonation, the solar Fenton method, photocatalytic degradation, and adsorption) have been investigated under a variety of experimental conditions (Alnajjar *et al.* 2007). Adsorption has numerous advantages over other conventional treatment methods because it is simple, inexpensive, and does not require the addition of nutrients (Lihme & Heegaard 2005).

Biochar (BC) is a solid product produced by the pyrolysis of biological organic material in an anoxic or anaerobic environment. BC can be used as a high-quality energy source, soil conditioner, reducing agent, slow-release carrier for fertilizers, and carbon dioxide sequestration agent. However, high costs are the main obstacle to using BC for large-scale wastewater treatment (Lehmann *et al.* 2011). The development of an affordable, broad-based, and rapidly renewable alternative adsorbent is therefore required (Spacie *et al.* 2011). Plant materials with unique environmental and cost advantages have been used to prepare new carbon materials with specific structures (Qi *et al.* 2016).

A wide range of plant material has been used to prepare BC (e.g., wild olive cores (Kaouah *et al.* 2013), papaya peel (Abbaszadeh *et al.* 2016), coffee grounds (Laksaci *et al.* 2017), and alligator weed (Kong *et al.* 2017)) and investigated under a variety of experimental conditions. The preparation of BC from *luffa* sponge as a raw material has been widely used in the adsorption of malachite green dye wastewater (Ang 2007), residual Cr(VI) (Miao *et al.* 2016), and phenol wastewater (Xiao *et al.* 2014); however, to the best of our knowledge, *luffa* sponge biochar for the removal of NOR residues in water has not been reported.

Luffa is widely cultivated in temperate and tropical regions around the world. Mature *luffa* forms a net fiber, called *luffa* sponge, that can be used for scrubbing and cleaning purposes as well as for medicinal use because of its diuretic properties to improve blood circulation and detoxification. *Luffa* is mainly composed of cellulose (82.4%), lignin (11.2%), and ash (0.4%), etc. (Tanobe *et al.* 2005). In addition, *luffa* has a uniquely porous physical structure, excellent mechanical strength, strong toughness, good acid and alkali properties (Akhtar *et al.* 2003; Vignoli *et al.* 2006; Ghali *et al.* 2009), and provides a good precondition for the preparation of biochar.

In this work, BC prepared from *luffa* sponge was used to adsorb NOR in synthetic wastewater. The BC was characterized based on its surface structure, specific surface area, porous structure, and Fourier-transform infrared (FTIR) spectrum (Mouille *et al.* 2003). Optimization of adsorption conditions was based on five factors: initial NOR concentration, pH, BC dosage, temperature, and contact time. Adsorption isotherm (Ozkaya 2006), adsorption kinetic (Chiron *et al.* 2003), and thermodynamic (Ghiorso & Sack 1995) models were used to study the adsorption mechanism.

MATERIALS AND METHOD

Starting material

Luffa sponge was purchased from a village in Jinan, China, and NOR (70458-96-7) from the Sangon Biological Engineering Corporation in Shanghai, China. The chemical formula of NOR is $C_{16}H_{18}FN_3O_3$, and its molecular weight is 319.33 g/mol. An initial NOR concentration of 100 mg/L was used.

Biochar preparation

Luffa sponge preparation first involved seed removal and cleaning with deionized (DI) water to remove dust. The *luffa* sponge was then dried at 70 °C for 2 days. Dried samples were crushed into 3- to 4-mm pieces using a high-speed grinder (HCP-100, Jinsui Company, Zhejiang). The broken samples were then infused with 85-wt% phosphoric acid at room temperature for 12 h at a solid-liquid ratio of 1:4 (g:mL) (Girgis & Ishak 1999). After activation, the samples were carbonized for 2 h in a box-type resistance furnace at 450 °C (Beijing Yongguang Company). The sample was then washed with DI water until the pH was close to 7. Once cooled, the sample was dried at 70 °C for 48 h and ground to a 200 mesh.

BC characterization

The surface area structure of the BC was observed using scanning electron microscopy (SEM) (Ory *et al.* 2006). The BC surface area and pore size were analyzed by

Brunauer–Emmett–Teller (BET). The effect of adsorption on BC functional groups was analyzed by FTIR. The BC sample and KBr powder were mixed evenly in the desired proportions, and then pressed into a piece, and scanned over the 4,000–400 cm^{-1} wavelength range.

Adsorption experiments

A UV spectrophotometer (T6-Xinshiji, Beijing) was used to detect different concentration gradients of the NOR solution at 271 nm (Ramsahye *et al.* 2007), and the standard concentration vs. absorbance curve was plotted to calculate additional NOR concentrations. A certain amount of BC was added to the NOR solution, and the mixture was agitated at a constant stirring velocity of 180 rpm in a temperature-controlled oscillator (HZQ-2, Jintan, Beijing). A 0.22-m filter membrane was used to filter the mixture in order to determine the absorbance. The standard deviation of each data point was calculated to ensure reliable experimental results. Each experimental batch consisted of three parallel runs and a blank. The equilibrium adsorption quantity (Q_e) (mg/g)] and removal rate (R) (%)] were calculated by Equations (1) and (2),

$$Q_e = \frac{(C_0 - C_e)V}{W} \tag{1}$$

$$R = \frac{(C_0 - C_e)}{C_0} \times 100 \tag{2}$$

where C_0 is the initial concentration (mg/L), C_e is the equilibrium concentration of NOR (mg/L), V is the volume of solution (L), and W is the quality of BC.

Adsorption isotherms

Different concentrations of NOR (50–200 mg/L) were mixed with a fixed amount of BC in a 100-ml conical bottle. The sample was stirred at a constant stirring speed of 180 rpm in an oscillator at a controlled temperature of 288, 298, or 303 K. The pH was regulated during the experiments using titrated Na(OH) and HCl to pH = 6.

Three isotherm models were used to evaluate the experimental results: the Langmuir (Dada 2012), Freundlich, and Dubinin-Radushkevich models (Desta 2013). The expression of the Langmuir model is as follows:

$$\frac{C_e}{Q_e} = \frac{1}{Q_m K_L} + \frac{C_e}{Q_m} \tag{3}$$

where Q_m (mg/g) is the maximum NOR adsorption capacity, and k_L (L/mg) is the Langmuir constant, which is associated with the energy of adsorption. The Freundlich equation can be used to describe multilayer adsorption according to:

$$\ln \mathrm{Q_e} = \ln \mathrm{K_F} + \frac{1}{\mathrm{n}} \ln \mathrm{C_e} \tag{4}$$

where K_F is the Freundlich constant (mg/g) and $1/n$ is the adsorption intensity. The Dubinin-Radushkevich model is given as:

$$lnQ_e = lnQ_m - \beta\varepsilon^2 \tag{5}$$

$$\varepsilon = RTln\left(1 + \frac{1}{C_e}\right) \tag{6}$$

$$E = \frac{1}{(2\beta)^{\frac{1}{2}}} \tag{7}$$

where R is the ideal gas constant (8.314 J/(mol K)), β is a constant corresponding to the adsorbed energy, ε is the Polanyi potential, T (K) is the thermodynamic temperature, and E (kJ/mol) is the average adsorption free energy.

Adsorption kinetics

We employ the three most widely-used kinetic models (pseudo-first-order, pseudo-second-order, and intraparticle diffusion) to analyze the adsorption kinetic data. The pseudo-first-order model can be expressed as:

$$\ln\ (Q_e - Q_t) = \ln Q_e K_1 t \tag{8}$$

where Q_t is the amount of adsorption at contact time t (min), and K_1 is the rate constant (min^{-1}).

The pseudo-second-order equation is expressed as:

$$\frac{\mathrm{t}}{\mathrm{Q_t}} = \frac{1}{\mathrm{K_2 Q_e^2}} + \frac{\mathrm{t}}{\mathrm{Q_e}} = \frac{1}{\mathrm{V_0}} + \frac{\mathrm{t}}{\mathrm{Q_e}} \tag{9}$$

where k_2 (g/(mg min)) is the rate constant and V_0 (mg g^{-1} min^{-1}) is the initial sorption rate.

The particle diffusion equation is expressed as:

$$Q_t = k_p t^{\frac{1}{2}} + C \tag{10}$$

where k_p (mg/(g min$^{1/2}$)) is the rate constant. Both k_p and C are calculated from the fitted line of Q_t against $t^{1/2}$.

Thermodynamics

Thermodynamic coefficients were determined from the 298–308 K adsorption experiments. Three parameters including the free energy change (ΔG), enthalpy change (ΔH), and entropy change (ΔS) were calculated as follows:

$$\ln K_L = \frac{\Delta S}{R} - \frac{\Delta H}{RT} \tag{11}$$

$$\Delta G = -RT ln K_L \tag{12}$$

RESULTS AND DISCUSSION

BC characteristics

Figures 1(a) and 1(b) were used to characterize the surface properties of *luffa* BC by SEM. Figure 1(a) clearly shows that the BC surface is rough and has a rich pore structure that forms after the activation of phosphoric acid when *luffa* undergoes high-temperature carbonization, which leads to internal etching and enhances bio-carbon adsorption. However, the SEM adsorption spectrum (Figure 1(b)) shows a reduced pore structure because the BC surface was filled by NOR molecules, which indicates that *luffa* BC is a good NOR adsorbent.

The BC pore structure distribution (Figure 2(a)) shows that most pores are mesopores (diameter: 2–10 nm), in addition to micropores (diameter: 0–2 nm). However, no macropores (diameter: 10–50 nm) were observed on the BC surface. The BET surface area of the BC was 822.35 m^2/g, and the mean aperture was 5.35 nm. The specific surface area and pore size have a strong and generally inverse relationship (Graber *et al.* 2012). The N_2 adsorption/desorption isotherm of the BC

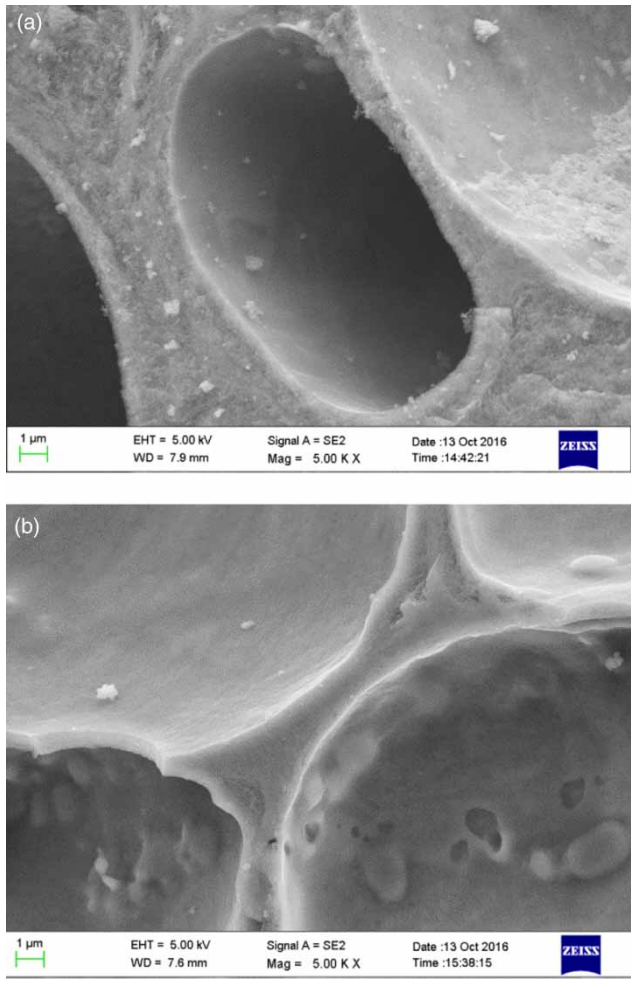

Figure 1 | Scanning electron microscope images of the biochar (a) before and (b) after norfloxacin adsorption.

(Figure 2(b)) exhibits a curve representative of a mixture of BC forms I and IV. This indicates that the gas adsorption rate rises quickly to a limit with increasing pressure in the low-pressure range, and a wide hysteresis loop appears at high pressure (Wang *et al.* 2013). This also indicates that the porous BC structure is a mixture of micropores and mesopores, which is advantageous for adsorption.

Experimental parameters

Effect of contact time

Figure 3(a) shows the effect on adsorption capacity and removal rates during a 0–360-minute contact time.

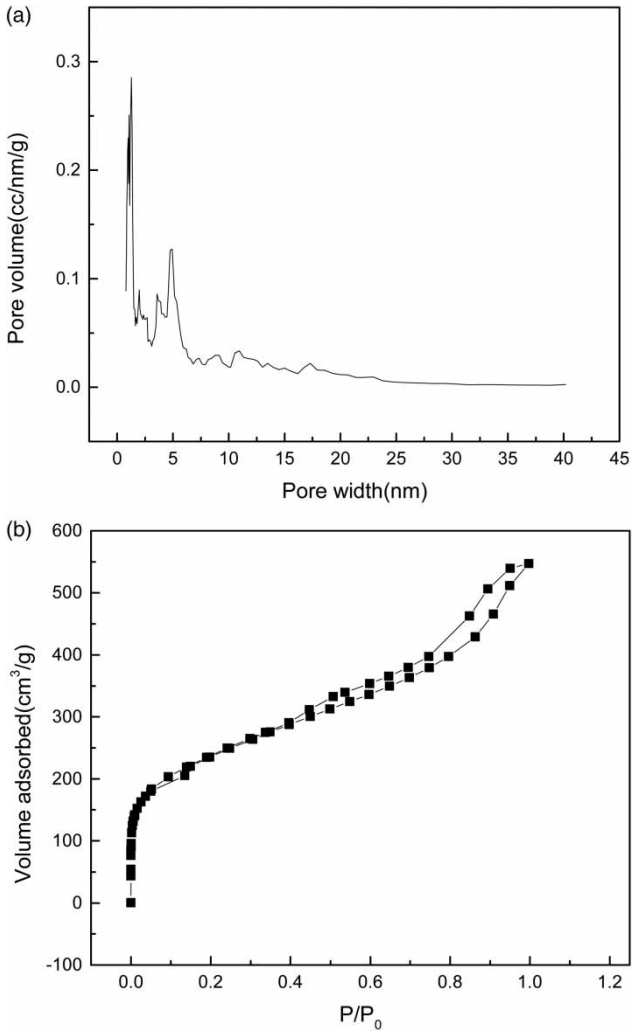

Figure 2 | (a) Pore size distribution and (b) N_2 adsorption isotherms of the biochar.

The removal rate rises rapidly from 59% (±0.97) to 83% (±0.37) in the first 60 minutes because of the adsorption of NOR molecules onto vacant active sites, which also provide a high driving force for the adsorption process in general (Kong *et al.* 2017). After 240 minutes, the removal rate becomes constant, indicating that adsorption has reached a balanced state. This occurs because the number of empty active sites gradually decreases with time, interaction between NOR molecules and internal particles produces repulsion (Nagda & Ghole 2009), and the BC surface becomes saturated with adsorbed NOR molecules (Li *et al.* 2009). The equilibrium time of BC adsorption of NOR is therefore 240 minutes.

Effect of temperature

Figure 3(b) shows the effect of temperature on the NOR removal rate and adsorption capacity. The removal rate and adsorption amount decrease slightly with increasing temperature from 96% (±0.80) to 95% (±0.60) and from 135 (±0.45) to 131 (±0.36) mg/g, respectively, which indicates that the adsorption process is exothermic (Kuzmichov & Pogorelov 2003). Previous studies showed that the adsorption properties of adsorbent molecules are enhanced under high-temperature conditions, which also supports that adsorption is exothermic. Adsorption efficiency tests can therefore be performed at room temperature.

Effect of BC content

The effect of BC dosage on the NOR removal rate and equilibrium adsorption amount is shown in Figure 3(c). Increasing the BC dosage from 0.1 to 0.6 g/L results in a rapid initial increase of the removal rate from 35% (±0.30) to 95% (±0.45). This implies that the number of adsorbed sites increases with increased amounts of BC, which reduces competition between NOR molecules (Xu *et al.* 2017). However, equilibrium adsorption decreases with increasing removal rate because as the removal rate approaches 100%, the limited remaining NOR solute molecules cannot be adsorbed onto more active sites, which results in more active-site vacancies (Kong *et al.* 2017). An adsorbent concentration of 0.5 g/L was therefore selected to maximize the effectiveness of *luffa* sponge.

Effect of initial solution pH

The initial aqueous solution pH places important controls over the adsorption process because it influences the surface charge and BC morphology (Cheng *et al.* 2008). The results indicate an optimum pH range of 5–7 (Figure 3(d)), for which the maximum adsorption capacity and removal rate were 128 mg/g (±0.300703) and 91% (±0.520833), respectively. The point of zero charge (pH_{pzc}) is an important parameter that indicates the influence of pH on adsorbent chemical characteristics and adsorption capacity. The determination of PZC of BC is shown in Figure 3(e). The pH_{pzc} for the BC was found to be about 1.8, Thereafter, the

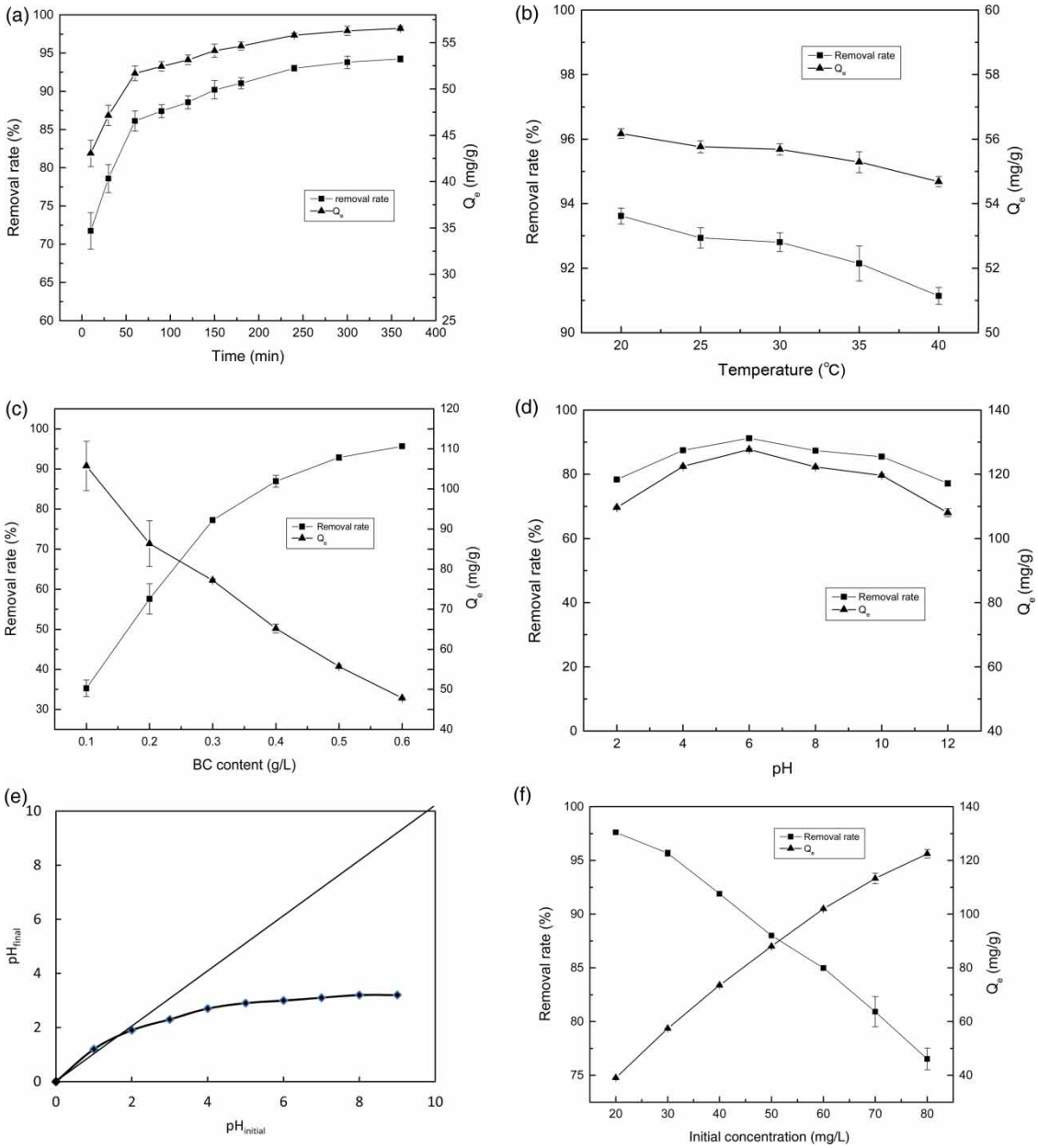

Figure 3 | Effects of the following factors on removal rate and adsorption capacity: (a) contact time; (b) temperature; (c) BC dosage; (d) solution pH; (e) pH_{pzc}; and (f) initial NOR concentration.

dissociation constant for the fluoroquinolones antibiotics have two ionization constant values at 5.45 and 6.2 (Bhatia *et al.* 2016). The cationic type dominates when pH <5.45 (László & Szűcs 2001), while the anionic type is dominant in pH >6.2. While the maximum adsorption capacity of NOR was at pH 6, the predominant species is the zwitterionic form. The adsorption of NOR was through electrostatic interactions and cation exchange, respectively (Adriano *et al.* 2006). This explains the improved adsorption at pH = 6.

Effect of initial concentration

Figure 3(f) shows that the removal efficiency decreases with increasing initial concentration from 92% (±0.601407) to

77% (±0.68306), and the adsorption capacity increases from 39 (±0.521301) to 121 (±0.491926) mg/g. The removal efficiency decreases because of the limited number of empty active sites and saturation at low concentrations. A large number of molecules therefore compete for limited surface sites (Qi *et al.* 2016). The adsorption quantity increases with increasing initial NOR concentration, but the adsorption efficiency does not improve because the number of active sites is insufficient to meet the demand of such a large number of molecules. An initial concentration of 30 mg/L was therefore used in subsequent experiments.

Adsorption mechanism analysis

Adsorption isotherms

The study of adsorption isotherms provides important information about the molecular adsorption performance and maximum adsorption capacity of BC. To determine the most suitable model for the NOR adsorption process using *luffa* sponge BC, the normalized standard deviation (Δq) was introduced, the Δq is calculated as follows:

$$\Delta q(\%) = 100\sqrt{\frac{\sum[(Q_{\exp} - Q_{\text{cal}})/Q_{\exp}]^2}{N-1}} \tag{13}$$

where $Q_{\exp}$ and Q_{cal} (mg/g) were measured by the experimental and model-calculated equilibrium adsorption quantities, respectively. Smaller Δq values indicate a smaller deviation between the calculated and measured data, and help to identify the model best suited for describing the adsorption process. In these experiments, three isotherm models were used to analyze the adsorption equilibrium data of nonlinear models, and the Freundlich isotherm model was adapted to better fit parameters of the three isothermal equations (Table 1). The correlation coefficient ($R^2 > 0.99$) simulated by the Freundlich model is higher than those of other isotherm models, and the Δq values of the Freundlich model are smaller than those of other models. The value of $1/n$ is less than 1, indicating a good adsorption effect. The results demonstrate that adsorption can be explained by a multilayer adsorption mechanism and occurs on heterogeneous surfaces (Cochrane *et al.* 2006). This heterogeneity can be attributed to various interactions of BC and functional groups on the BC surface. The maximum adsorption (250 mg/g) of NOR by *luffa* is higher than that of different adsorbents, as shown in Table 2. The dates show that the maximum adsorption capacity of BC of *luffa* is higher than that of other adsorbent materials, which suggests that the *luffa* sponge can be used to prepare BC with high adsorption efficiency.

Adsorption kinetics

The adsorption kinetics data were fitted with pseudo-first-order, pseudo-second-order, and intraparticle diffusion models to determine the adsorption mechanism. The optimal adsorption kinetic model was determined by a combination of the normalized standard deviation Δq (%) and correlation coefficient R^2. Fitted parameters of the three kinetic models are listed in Table 3. The correlation coefficient ($R^2 > 0.99$) simulated by the pseudo-second-order model is higher than those of other models, and the Δq values are smaller than those of other models. Additionally, the results show that the pseudo-second-order model (Q_e) best fits the Q_{exp} data, indicating that the pseudo-second-order model can well fit the adsorption process of the BC to NOR solution. Thus, the adsorption rate is

Table 1 | Correlation parameters for the Langmuir, Freundlich, and Dubinin-Radushkevich models

	Langmuir model				Freundlich model			Dubinin-Radushkevich model					
Temperature (K)	Q_m (mg/g)	K_L (L/mg)	R^2	Δq (%)	$1/n$	K_F (mg/g)$^{1/n}$	R^2	Δq (%)	β (mol^2/J^2)	Q_m (mg/g)	E (KJ/mol)	R^2	Δq (%)
288	286	0.2614	0.9881	6.734	0.1113	146.9217	0.9984	3.976	3×10^{-6}	244	408	0.928	10.156
298	278	0.2034	0.9872	6.671	0.1410	142.7079	0.9918	5.432	1×10^{-6}	245	707	0.8762	15.476
308	250	0.3333	0.9867	5.319	0.1449	151.1995	0.9995	2.312	6×10^{-6}	272	289	0.8904	14.69

Table 2 | Comparison of *luffa* sponge with other adsorbents

Adsorbent	Adsorbate	Maximum adsorption capacity (mg/g)	References
Luffa sponge	Norfloxacin	250	This work
Papaya peel	Pb	38	Abbaszadeh *et al.* (2016)
Pine leaves	Hazardous azo dye	71.94	Deniz & Saygideger (2011)
C-MWCNT[a]	Norfloxacin	89.3	Yang *et al.* (2012)
Bentonite	Basic Yellow 28	208.3	Turabik (2008)

[a]Carboxylated multiwall carbon nanotube.

controlled by chemical adsorption of valence forces by exchanging or sharing electrons between the adsorbent and NOR molecules (Rogachev 2008; Mahmoud *et al.* 2016).

Thermodynamics

Calculated Gibbs free energy, entropy, and enthalpy values are listed in Table 4. The ΔG indicates that the degree of spontaneity and adsorption of NOR were feasible, and more negative ΔG values produced a better adsorption effect, indicating spontaneous adsorption (Abbaszadeh *et al.* 2016). The free energy decreases with increasing temperature, which leads to decreased adsorption rates at high temperature. The negative ΔH value confirms that adsorption is exothermic, which is consistent with the increased adsorption capacity observed in the Langmuir isotherm model with decreasing temperature. Additionally, the temperature effect also confirmed that the BC adsorption NOR process is exothermic process. The ΔS value is negative, which also indicates that randomness reduces adsorption.

FTIR

The FTIR spectra of BC before and after NOR adsorption are shown in Figure 4. The types of surface functional groups changed very little before and after BC adsorption. The spectral peak at 400–500 cm^{-1} was observed before adsorption, due to the vibration of a metal-oxygen and metal-hydroxyl, but disappeared after the NOR biosorption by BC (Puziy *et al.* 2003). The peak at 1,080–1,800 cm^{-1} indicates that the surface of the bio-carbon contains phosphorus functional groups due to pretreatment with phosphoric acid (Kaouah *et al.* 2013). The absorption peak at 1,570 cm^{-1} is caused by contraction vibrations of the aromatic ring. The 1,600 cm^{-1} peak is related to tensile vibration of the benzene ring or C = C bond (Shanmugharaj *et al.* 2007). The peak at 1,700 cm^{-1} is due to the vibration of C = O bonds in the carboxyl or conjugate carbonyl group (Seredych *et al.* 2009). Absorption peaks at 3,420 cm^{-1} are derived from the elastic vibrations of –OH bonds in the carboxyl, phenol hydroxyl, and water molecules (Laksaci *et al.* 2017). Figure 4 shows that the peak strength of BC decreased slightly after adsorption. It is shown that the surface groups of BC are involved in the process of adsorption of NOR, and they interact with NOR or are masked by NOR molecules.

Future research ideas

Luffa was widely cultivated in developing countries as an environmentally friendly biomaterial in eastern Asia and South America (Demir *et al.* 2008). Because of the high yield and easy availability of *luffa*, *luffa* sponge can be prepared into low cost biochar. Commercial activated carbon is usually used to remove contaminants from water. However, commercial activated carbon is expensive, leading to a higher cost of wastewater treatment (the cost of commercial activated carbon is CN¥ 10.4/kg). The study of our research team showed the cost of production of *luffa* sponges biochar is CN¥ 2.1/kg. Therefore, use of *luffa* biochar can greatly reduce the cost of the water treatment field. This greatly reduces the cost of water treatment areas and facilitates economic diversification in developing countries. In addition, there are many areas where biochar can be applied. Biochar can also improve soil fertility (Yuan *et al.* 2018) and soil mechanisms (Khan *et al.* 2016)

Table 3 | Parameters for three kinetic models of NOR adsorption

Concentration (mg/l)	Exp-data Qe (mg/g)	Pseudo-first-order kinetics				Pseudo-second-order kinetics				Particle diffusion model			
		K_1 (min^{-1})	Q_e (mg/g)	R^2	Δq (%)	K_2 ($g.mg^{-1}.g^{-1}$)	Q_e (mg/g)	V_0 ($mg.g^{-1}.min^{-1}$)	R^2	Δq (%)	K_p ($mg.g^{-1}.min^{-1/2}$)	C (mg/g)	R^2	Δq (%)
100	122	0.0176	70	0.9939	11.61	0.00056	121	33.22	0.9998	5.63	3.9321	175.54	0.8852	24.78
150	147	0.0128	88	0.9760	17.42	0.00030	144	18.98	0.9989	9.76	4.9177	160.75	0.9809	17.43
200	176	0.0277	150	0.9842	15.74	0.00033	178	24.10	0.9996	3.28	6.2697	161.16	0.8663	29.67

Table 4 | Thermodynamic parameters for NOR adsorption on BC

T (K)	K (L/mol)	△G (kJ/mol)	△S (J/mol K)	△H (kJ/mol)
288	118,837	−27.98		
298	92,451	−28.33	−126	−8.6
308	151,515	−30.55		

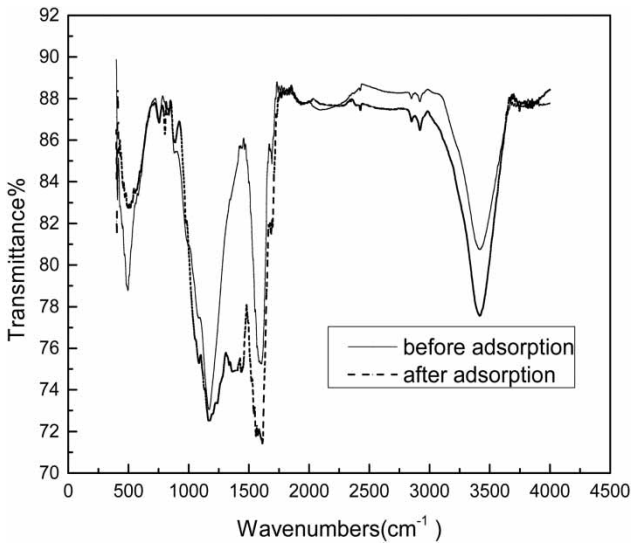

Figure 4 | FTIR spectra of the BC before and after NOR adsorption.

while treating soil contaminants (Khorram *et al.* 2018). Moreover, biochar can affect the mitigation of greenhouse gas emissions (Li *et al.* 2018). Thus, BC has great significance and wider application prospects in global carbon biogeochemical cycling, mitigation of global climate change research and ecological remediation of pollutants.

CONCLUSIONS

BC derived from *luffa* sponge is an effective low-cost material for removing NOR from aqueous wastewater. SEM analyses show that the adsorbent has a coarse surface with a well-developed porous structure containing abundant micropores and mesopores. The BC surface area is high (822.35 m^2/g), and the average pore size is 5.35 nm. These physical characteristics indicate that BC has excellent properties for NOR adsorption. The maximum adsorption capacity of the BC was 250 mg/g. Batch adsorption studies

were performed to evaluate the ability of BC to remove NOR from aqueous solutions. The NOR adsorption kinetic data correlate well with a pseudo-second-order kinetic model, with a high R^2 (>0.99), which shows that chemisorption is the rate-limiting factor. The experimental data are best described by the Freundlich isotherm model ($R^2 >$ 0.99), which indicates multilayer adsorption. The thermodynamic parameters show that adsorption is exothermal and spontaneous. The FTIR spectra indicate that the BC surface has more acidic oxygen-containing groups such as carboxyl, phenol hydroxyl, lactone, and carbonyl. Because *luffa* sponge is inexpensive and easy to obtain, this technology offers broad application prospects to manage wastewater clean-up.

ACKNOWLEDGEMENTS

This work was supported by the International Postdoctoral Exchange Fellowship Program (No. 20180063), National Natural Science Foundation of China (No. 51708340), Major Science and Technology Program for Water Pollution Control and Treatment (2017ZX07101-001), Promotional Research Fund for Excellent Young and Middle-aged Scientists of Shandong Province (ZR2016CB18 and ZR2015DM012) and Project of Shandong Province Higher Educational Science and Technology Program (No. J15LE07 and No. J14LD02).

REFERENCES

Abbaszadeh, S., Alwi, S. R. W., Webb, C., Ghasemi, N. & Muhamad, I. I. 2016 Treatment of lead-contaminated water using activated carbon adsorbent from locally available papaya peel biowaste. *Journal of Cleaner Production* **118**, 210–222.

Adriano, W. S., Veredas, V., Santana, C. C. & Gonçalves, L. R. B. 2006 Adsorption of amoxicillin on chitosan beads: kinetics, equilibrium and validation of finite bath models. *Biochemical Engineering Journal* **27** (2), 132–137.

Akhtar, N., Saeed, A. & Iqbal, M. 2003 Chlorella sorokiniana immobilized on the biomatrix of vegetable sponge of *luffa* cylindrica: a new system to remove cadmium from contaminated aqueous medium. *Bioresource Technology* **88** (2), 163–165.

Alnajjar, A., Idris, A. M. & Abuseada, H. H. 2007 Development of a stability-indicating capillary electrophoresis method for norfloxacin and its inactive decarboxylated degradant. *Microchemical Journal* **87** (1), 35–40.

Ang, E. L. 2007 Removal of malachite green from aqueous solution by adsorption using luffa sponge biomass. http://eprints.ums.edu.my/8173/ (accessed 25 July 2018).

Bhatia, V., Ray, A. K. & Dhir, A. 2016 Enhanced photocatalytic degradation of ofloxacin by co-doped titanium dioxide under solar irradiation. *Separation & Purification Technology* **161**, 1–7.

Boerner, R. J., Sommer, H., Berger, W., Kuhn, U., Schmidt, U. & Mannel, M. 2003 Kava-kava extract Li 150 is as effective as opipramol and buspirone in generalised anxiety disorder –an 8-week randomized, double-blind multi-centre clinical trial in 129 out-patients. *Phytomedicine* **10** (1), 38–49.

Cheng, C. H., Lehmann, J. & Engelhard, M. H. 2008 Natural oxidation of black carbon in soils: changes in molecular form and surface charge along a climosequence. *Geochimica Et Cosmochimica Acta* **72** (6), 1598–1610.

Chiron, N., Guilet, R. & Deydier, E. 2003 Adsorption of Cu(II) and Pb(II) onto a grafted silica: isotherms and kinetic models. *Water Research* **37** (13), 3079–3086.

Cochrane, E. L., Lu, S., Gibb, S. W. & Villaescusa, I. 2006 A comparison of low-cost biosorbents and commercial sorbents for the removal of copper from aqueous media. *Journal of Hazardous Materials* **137** (1), 198–206.

Dada, A. O. 2012 Langmuir, Freundlich, Temkin and Dubinin–Radushkevich isotherms studies of equilibrium sorption of Zn^{2+} unto phosphoric acid modified rice husk. *IOSR Journal of Applied Chemistry* **3** (1), 38–45.

Demir, H., Top, A., Balköse, D. & Ülkü, S. 2008 Dye adsorption behavior of luffa cylindrica, fibers. *Journal of Hazardous Materials* **153** (1–2), 389–394.

Deniz, F. & Saygideger, S. D. 2011 Removal of a hazardous azo dye (basic red 46) from aqueous solution by princess tree leaf. *Desalination* **268**, 6–11.

Desta, M. B. 2013 Batch sorption experiments: Langmuir and Freundlich isotherm studies for the adsorption of textile metal ions onto Teff straw (*Eragrostis* tef) agricultural waste. *Journal of Thermodynamics* **2013** (1), 6.

Ghali, L., Msahli, S., Zidi, M. & Sakli, F. 2009 Effect of pre-treatment of luffa fibres on the structural properties. *Materials Letters* **63** (1), 61–63.

Ghiorso, M. S. & Sack, R. O. 1995 Chemical mass transfer in magmatic processes IV. A revised and internally consistent thermodynamic model for the interpolation and extrapolation of liquid-solid equilibria in magmatic systems at elevated temperatures and pressures. *Contributions to Mineralogy & Petrology* **119** (2–3), 197–212.

Girgis, B. S. & Ishak, M. F. 1999 Activated carbon from cotton stalks by impregnation with phosphoric acid. *Materials Letters* **39** (2), 107–114.

Graber, E. R., Tsechansky, L., Gerstl, Z. & Lew, B. 2012 High surface area biochar negatively impacts herbicide efficacy. *Plant & Soil* **353** (1–2), 95–106.

Hallingsørensen, B., Nors, N. S., Lanzky, P. F., Ingerslev, F., Holten Lützhøft, H. C. & Jørgensen, S. E. 1998 Occurrence, fate and effects of pharmaceutical substances in the environment – a review. *Chemosphere* **36** (2), 357.

Holmes, B., Brogden, R. N. & Richards, D. M. 1985 Norfloxacin. *Drugs* **30** (6), 482–513.

Kaouah, F., Boumaza, S., Berrama, T., Trari, M. & Bendjama, Z. 2013 Preparation and characterization of activated carbon from wild olive cores (oleaster) by H_3PO_4, for the removal of basic red 46. *Journal of Cleaner Production* **54** (8), 296–306.

Khan, K. T., Chowdhury, M. & Huq, S. I. 2016 Application of biochar and fate of soil nutrients. *Bangladesh Journal of Scientific Research* **27** (1), 11.

Khorram, M. S., Sarmah, A. K. & Yu, Y. 2018 The effects of biochar properties on fomesafen adsorption-desorption capacity of biochar-amended soil. *Water Air & Soil Pollution* **229** (3), 60.

Kong, Q., Wang, Y., Li, S. & Miao, M. S. 2016 Isotherm, kinetic, and thermodynamic equations for cefalexin removal from liquids using activated carbon synthesized from loofah sponge. *Desalination & Water Treatment* **57** (17), 7933–7942.

Kong, Q., Liu, Q., Miao, M. S., Liu, Y. Z., Chen, Q. F. & Zhao, C. S. 2017 Kinetic and equilibrium studies of the biosorption of sunset yellow dye by alligator weed activated carbon. *Desalination & Water Treatment* **66**, 281–290.

Kuzmichov, V. M. & Pogorelov, S. V. 2003 Improving the accuracy of temperature dependence measurements for the absorption efficiency factor in platinum bolometers. *Telecommunications & Radio Engineering* **60**, 104–107.

Laksaci, H., Khelifi, A., Trari, M. & Addoun, A. 2017 Synthesis and characterization of microporous activated carbon from coffee grounds using potassium hydroxides. *Journal of Cleaner Production* **147**, 254–262.

László, K. & Szűcs, A. 2001 Surface characterization of polyethyleneterephthalate (PET) based activated carbon and the effect of pH on its adsorption capacity from aqueous phenol and 2,3,4-trichlorophenol solutions. *Carbon* **39** (13), 1945–1953.

Lehmann, J., Rillig, M. C., Thies, J., Masiello, C. A., Hockaday, W. C. & Crowley, D. 2011 Biochar effects on soil biota –a review. *Soil Biology & Biochemistry* **43** (9), 1812–1836.

Li, W., Wang, N., Chen, J., Liu, G., Pan, Z. & Guan, Y. 2009 Quantitative study of interior nanostructure in hollow zinc oxide particles on the basis of nondestructive x-ray nanotomography. *Applied Physics Letters* **95** (5), 3309.

Li, Y., Hu, S., Chen, J., Müller, K., Li, Y., Fu, W., Lin, Z. & Wang, H. 2018 Effects of biochar application in forest ecosystems on soil properties and greenhouse gas emissions: a review. *Journal of Soils & Sediments* **18** (2), 546–563.

Lihme, A. O. F. & Heegaard, P. M. H. 2005 Extracorporeal stabilised expanded bed adsorption method for the treatment of sepsis. *EP* **34** (4), 514–515.

Mahmoud, M. E., Nabil, G. M., El-Mallah, N. M., Bassiouny, H. I., Kumar, S. & Abdel-Fattah, T. M. 2016 Kinetics, isotherm, and thermodynamic studies of the adsorption of reactive red 195 a dye from water by modified switchgrass biochar adsorbent. *Journal of Industrial & Engineering Chemistry* **37**, 156–167.

Miao, M., Wang, Y., Kong, Q. & Shu, L. 2016 Adsorption kinetics and optimum conditions for Cr(VI) removal by activated carbon prepared from luffa sponge. *Desalination & Water Treatment* **57** (17), 7763–7772.

Mouille, G., Robin, S., Lecomte, M., Pagant, S. & Höfte, H. 2003 Classification and identification of *arabidopsis* cell wall mutants using Fourier-Transform InfraRed (FTIR) microspectroscopy. *Plant Journal for Cell & Molecular Biology* **35** (3), 393–404.

Nagda, G. K. & Ghole, V. S. 2009 Biosorption of Congo red by hydrogen peroxide treated tendu waste. *Iranian Journal of Environmental Health Science & Engineering* **6** (3), 195–200.

Ory, Z., Elisha, M. & Stepphan, T. 2006 Device and method for the examination of samples in a non-vacuum environment using a scanning electron microscope: US, US 6992300 B2 [P].

Ozkaya, B. 2006 Adsorption and desorption of phenol on activated carbon and a comparison of isotherm models. *Journal of Hazardous Materials* **129** (1–3), 158.

Puziy, A. M., Poddubnaya, O. I., Martínez-Alonso, A., Suárez-García, F. & Tascón, J. M. D. 2003 Synthetic carbons activated with phosphoric acid III. Carbons prepared in air. *Carbon* **41**, 1181–1191.

Qi, Z., Liu, Q., Zhu, Z. R., Kong, Q., Chen, Q. F., Zhao, C. S., Miao, M. S. & Wang, C. 2016 Rhodamine b removal from aqueous solutions using loofah sponge and activated carbon prepared from loofah sponge. *Desalination & Water Treatment* **57**, 1–13.

Ramsahye, N. A., Maurin, G., Bourrelly, S., Llewellyn, P. L., Loiseau, T. & Serre, C. 2007 On the breathing effect of a metal-organic framework upon Co(2) adsorption: monte carlo compared to microcalorimetry experiments. *Chemical Communications* **31** (31), 3261.

Rogachev, A. S. 2008 Cheminform abstract: exothermic reaction waves in multilayer nanofilms. *ChemInform* **39** (26), 176–182.

Seredych, M., Merwe, M. V. D. & Bandosz, T. J. 2009 Effects of surface chemistry on the reactive adsorption of hydrogen cyanide on activated carbons. *Carbon* **47** (10), 2456–2465.

Shanmugharaj, A., Bae, J., Lee, K., Noh, W., Lee, S. & Ryu, S. 2007 Physical and chemical characteristics of multiwalled carbon nanotubes functionalized with aminosilane and its influence on the properties of natural rubber composites. *Composites Science & Technology* **67**, 1813–1822.

Spacie, C. J., Davies, R. K. & Stirling, C. A. 2011 Carbon materials: US, US8034451[P].

Tanobe, V. O. A., Sydenstricker, T. H. D., Munaro, M. & Amico, S. C. 2005 A comprehensive characterization of chemically treated Brazilian sponge-gourds (*luffa* cylindrica). *Polymer Testing* **24** (4), 474–482.

Turabik, M. 2008 Adsorption of basic dyes from single and binary component systems onto bentonite: simultaneous analysis of basic red 46 and basic yellow 28 by first order derivative

spectrophotometric analysis method. *Journal of Hazardous Materials* **158** (1), 52–64.

Vignoli, J. A., Cetligoi, M. P. C. & Silva, R. S. E. 2006 Development of a statistical model for sorbitol production by free and immobilized *Zymomonas* mobilis in loofa sponge Luffa cylindrica. *Process Biochemistry* **41** (1), 240–243.

Wang, B., Li, C. & Hui, L. 2013 Bioleaching of heavy metal from woody biochar using *acidithiobacillus* ferrooxidans, and activation for adsorption. *Bioresource Technology* **146** (10), 803.

Xiao, X., Xu, D., Chen, Z., Xu, S. & Xia, S. 2014 Study on phenol adsorption capacity by activated carbon fiber based on luffa sponge fiber. *Industrial Water Treatment* **34** (4), 22–25.

Xu, F., Qi, X. Y., Kong, Q., Shu, L., Miao, M. S., Xu, S. G., Du, Y. D., Wang, Q., Liu, Q. & Ma, S. S. 2017 Adsorption of sunset yellow by *luffa* sponge, modified luffa and activated carbon from *luffa* sponge. *Desalination & Water Treatment* **96**, 86–96.

Yang, W., Lu, Y., Zheng, F., Xue, X., Li, N. & Liu, D. 2012 Adsorption behavior and mechanisms of norfloxacin onto porous resins and carbon nanotube. *Chemical Engineering Journal* **179** (1), 112–118.

Yuan, J., Tong, Y., Lu, S. & Yuan, G. 2018 Comprehensive evaluation on soil fertility quality of jujube orchard under combined application of biochar and nitrogen fertilizer. *Transactions of the Chinese Society of Agricultural Engineering* **34** (1), 134–140.

First received 12 April 2018; accepted in revised form 1 August 2018. Available online 27 August 2018